scientific reports

Check for updates

OPEN

Bone mesenchymal stem cells based on matric hydrogels attenuate intervertebral disc degeneration by suppressing oxidative stress-induced ferroptosis

Song Fu[1], Renhua Lv[2], Longqiang Wang[1], Zhenyu Wang[1], Fengming Wang[1], Hao Gao[1], Wei Zhao[1], Xiaoling Huang[1], Xiaojun Li[1] & Yanan Wang[1]✉

Intervertebral disc degeneration (IVDD) and its attendant lower back pain are a major medical challenge. Ferroptosis has become a new target for the treatment of IVDD. Mesenchymal stem cells (MSCs) are a promising regenerative therapy for IVDD. Hydrogel is usually used as a delivery carrier for MSCs. This study investigated the effect of bone mesenchymal stem cells (BMSCs) in IVDD by magnetic resonance imaging (MRI) and hematoxylin and eosin (HE) staining analysis using a rat-punctured IVDD model. A vitro model of tert-butyl hydroperoxide (TBHP)-induced oxidative stress injury in annulus fibrosus cells (AFCs) was used to explore the underlying molecular mechanisms. Cell viability was detected by cell counting kit-8 assay. Ferroptosis was assessed by measuring the levels of LDH, Fe^{2+}, glutathione, lipid reactive oxygen species, and malondialdehyde. The underlying mechanism was investigated by western blot and phosphor-kinase array. Results suggested that BMSCs inhibited TBHP-induced ferroptosis and the phosphorylated levels of STAT3 in AFCs. The activation of STAT3 (colivelin, a specific agonist for STAT3) reversed the effects on the ferroptosis of BMSCs. Additionally, BMSCs alleviated IVDD progression based on matrix hydrogels, while colivelin abolished the protective effects of BMSCs-encapsulated hydrogels on IVDD. In short, BMSCs inhibited oxidative stress-induced AFCs ferroptosis, thereby alleviating IVDD, which is associated with inhibited STAT3 activation. This study demonstrated the possible underlying mechanism by which BMSCs mitigate IVDD and may provide a new therapeutic idea for IVDD.

Keywords Intervertebral disc degeneration, Bone mesenchymal stem cell, Matric hydrogels, Ferroptosis, STAT3

In the world today, more than four-fifths of the population suffers from chronic lower back pain caused primarily by intervertebral disc degeneration (IVDD)[1]. IVDD is a common degenerative disease of skeletal muscle that worsens with age, leading to a significant financial burden on families. The main characteristics of IVDD are disc dehydration and collapse, annulus fibrosus (AF) rupture, extracellular matrix (ECM) changes, and proteoglycan loss in the nucleus pulposus (NP)[2]. At present, surgical and conservative treatment of IVDD can only alleviate the symptoms of disc degeneration, but cannot prevent or reverse the progression of IVDD[3]. Despite rapid advances in genetic engineering technology[4]and stem cell therapies[5], their use to treat IVDD has been limited, possibly due to the unelucidated mechanisms of action.

Stem cells (SCs) are isolated from different sources, such as adipose tissues, umbilical cord, and bone marrow[6]. A variety of SCs have been successfully transplanted into intervertebral discs (IVDs) to repair or regenerate the IVDD, including muscle-derived stem cells, hematopoietic stem cells, adipose stem cells (ASCs), bone marrow mesenchymal stem cells (BMSCs) and synovial stem cells[7]. In particular, BMSCs have anti-angiogenesis, anti-apoptosis, anti-fibrosis, anti-inflammatory, regenerative, and immunomodulatory abilities[8]. Besides, the ability of BMSCs to differentiate into adipocytes, osteoblasts, and chondroblasts in vitro has attracted much

[1]Department of Minimally Invasive Spine Surgery, Shandong Wendeng Orthopedic Hospital, No.1, Fengshan Road, Wendeng District, Weihai 264400, Shandong Province, China. [2]Department of Neurology, Weihai Central Hospital, Weihai, Shandong Province, China. ✉email: yanan1987@fjmu.edu.cn

attention[9]. NP and AF are important targets for regenerative therapy of disc degeneration, and inhibition of their pathological changes can significantly alleviate IVDD. BMSCs have been reported to have the potential to differentiate NP-like phenotypes to increase disc height and alleviate disc degeneration[10]. Therefore, it is reasonable and feasible to delay and treat IVDD by local BMSC transplantation. However, BMSCs-mediated functions in annulus fibrosus cells (AFCs) need further study.

Affected by the local microenvironment, it is difficult for SCs to survive when transplanted to the diseased sites, so the main challenge at present is to retain and stabilize them in vivo and improve their survival rate[11]. Injectable hydrogels as an ideal and effective scaffold material not only provide structural and mechanical support for degenerated IVD but also serve as delivery carriers for MSCs and other bioactive factors[12]. Notably, when hydrogels are used as stem cell carriers, they not only regulate the function of SCs and mimic the ECM but also have beneficial effects on cell survival and repair of cartilage tissues. Temperature-controlled hydrogels can quickly form gels at 37 °C, thus stopping cell flow[13]. Hydrogels have good biocompatibility and encapsulation ability, maintain small molecule biological activity, respect cell morphology and function, and provide a good growth local microenvironment for cells[14]. Therefore, co-implantation of SCs in combination with injectable hydrogels is currently being investigated as a potential NP therapy[15]. However, their repair function on AF has been fully unelucidated. Therefore, further investigation is needed to clarify the role of hydrogel-encapsulated BMSCs in AF repair.

Herein, we explored the effect of hydrogel-encapsulated BMSCs on IVDD in vivo, as well as used in vitro models to clarify the molecular mechanism of BMSCs. Specifically, we found that obstruction of IVDD progression by combination therapy with matrix hydrogels and BMSCs was closely associated with inhibition of the JAK2/STAT3 pathway and ferroptosis in AFCs.

Methods

Culture and identification of BMSCs

BMSCs belong to mesenchymal stem cells (MSCs) and possess multipotent differentiation potential. They are primarily isolated from bone marrow, typically obtained through bone marrow aspiration from the iliac crest. The BMSCs were purchased from the Chinese Academy of Science (Shanghai, China). BMSCs were cultured with a DMEM/F12 medium (Gibco BRL, Grand Island, NY, USA) containing 10% Fetal Bovine Serum (FBS; Gibco BRL) and 1% penicillin-streptomycin (Gibco BRL) at 37 °C, 5% CO_2, and 90% humidity. The medium changes were performed every two to three days. When cell density reached more than 90%, 0.25% trypsin/EDTA (1 mM, Gibco) was added to the medium and incubated for 3 min at 37 °C for digestion. The cells at passage two or three were used for follow-up experiments.

Following the manufacturer's protocols, the BMSCs surface markers were detected by positive expression of CD105 (CD105-FITC, BD Biosciences) and negative expression of CD34 (CD34-PE, BD Biosciences) by flow cytometry.

Oil Red O, Alizarin Red, and alkaline phosphatase (ALP) staining were performed to detect the adipogenic and osteogenic chondrogenic abilities of BMSCs. The Sprague-Dawley (SD) rat BMSCs osteogenesis and adipogenesis differentiation kits were obtained from Cyagen Biotech (Jiangsu, China). In short, BMSCs were digested to make cell suspension using 0.25% trypsin. The cell suspension was inoculated on six-well plates with a density of 1×10^5 cells/well until complete fusion. The relevant reagents were added proportionally to the base medium to prepare the lipogenic induction and osteogenic differentiation mediums respectively following the manufacturer's instructions. The cell was added to the medium and incubated for 3–4 weeks. The medium was replaced every three days. Finally, the cell was fixed with 4% paraformaldehyde, and subsequently stained with Oil Red O, Alizarin Red, and ALP, respectively.

Culture and treatment of annulus fibrosus cells (AFCs)

AFCs are the main cell type in the annulus fibrosus of the intervertebral disc and are responsible for maintaining the structure and function of the annulus fibrosus. They are primarily isolated from the annulus fibrosus tissue of the intervertebral disc. Pricella Biotechnology (Wuhan, China) supplied the rat intervertebral disc AFCs. The AFC cultured in DMEM/F12 containing 10% FBS and 1% penicillin-streptomycin at 37 °C with 5% CO_2. The cells in the second passage were used in subsequent experiments. Afterward, AFCs were divided into four groups: AFCs group, tert-butyl hydroperoxide (TBHP) group, TBHP + BMSCs group, and TBHP + BMSCs + colivelin group. AFCs were exposed to 100 μM TBHP (Sigma-Aldrich) for 3 h to establish the cell model. These AFCs were co-cultured with 1×10^5 cells/well BMSCs. To activate STAT3, the cells were treated with the STAT3-specific agonist colivelin (0.5 μM, MCE, Shanghai, China) or no treatment for 12 h.

Preparation of matrix hydrogels

The preparation method of matrix hydrogels was referred to by Roughley Peter et al.[16]. Ultrapure chitosan (BioSyntech, Laval, Canada) was dissolved in 0.1 mol/L hydrochloric acid overnight and then sterilized by autoclave. β-glycerophosphate (GP) was prepared in deionized water and then filtered through a 0.22 mm membrane. Finally, GP was dripped into the stirred chitosan solution and mixed, resulting in a mixture containing 2% w/w chitosan and 8% w/w GP. This chitosan solution turned into gels when heated to 37 °C.

Preparation of BMSCs embedded gel: BMSCs from passage three were digested using 0.25% trypsin and suspended in DMEM/F12 containing 10% FBS. Gently mix the gel solution with an equal volume of cell suspension at 4 °C. Then the mixture was cured at 37℃ for 20 min and gelled. The result obtains BMSC-embedded hydrogels with 1% chitosan containing 1×10^6 cells.

Cell viability

Following the manufacturer's protocols, cell-counting kit-8 (CCK-8; Beyotime, Shanghai, China) was performed to analyze the cell viability. In a word, AFCs (5×10^3 cells/well) were seeded to 96-well plates, processed with 10 μl 10% CCK-8 reagent, and incubated for 2 h at 37℃. The absorbance at 450 nm in each period was measured by a microplate reader (BMG Labtech, Offenburg, Germany).

Measurement of lactate dehydrogenase (LDH) content, Fe^{2+}, malondialdehyde (MDA), and glutathione (GSH) levels

The concentrations of LDH, Fe^{2+}, MDA, and GSH were assessed using a cytotoxicity LDH assay kit (Dojindo Laboratories, Shanghai, China), a Fe^{2+} detection kit (Solarbio, Beijing, China), an MDA detection kit (Sigma-Aldrich), and a GSH detection kit (Solarbio) following to the manufacturer's protocols.

Measurement of lipid reactive oxygen species (ROS)

To detect the level of lipid ROS, the cells seeded in a 6-well plate were cultured in a serum-free medium containing 5 μmol/L BODIPY C11 (D3861, Invitrogen) protected from light for 30 min at 37℃. Then, the cells were washed three times with PBS to remove excess BODIPY C11 solution and covered with DMEM. The fluorescence microscope measured the fluorescent signals at an emission wavelength of 593 nm and an excitation wavelength of 582 nm. The green fluorescence intensity that indicates the amount of lipid ROS was calculated using ImageJ software.

Phospho-kinase array

According to the manufacturer's manual, the relative levels of phosphorylation of multiple kinase phosphorylation sites were simultaneously measured using the Proteome Profiler Human Phospho-Kinase Array kit (R&D Systems, Minneapolis, MN, USA). Briefly, AFCs (1×10^7 cells/ml) were lysed with the lysis buffer on ice. The concentration of protein in the supernatants was detected after vibration and centrifugation. Next, the cell lysates were mixed with the biotinylated detection antibodies. The mixture was incubated with membranes contained with capture and control antibodies overnight. After washing the membrane the next day, streptavidin-horseradish peroxidase and chemiluminescent detection reagents were applied. A signal corresponding to the amount of phosphorylated protein binding is generated at each capture point. Pixel densities can be analyzed using image J analysis software.

Western blot

Total protein was extracted from indicated cells with lysis buffer (radioimmunoprecipitation assay buffer and proteinase inhibitor.) and its concentration was quantified using the BCA protein assay kit (Solarbio). The protein (30 μg) was separated by a 10% SDS-PAGE and then electroblotted to the PVDF membrane. The PVDF membrane was blocked with 5% skim milk or TBST containing 5% BSA at room temperature for 2 h. and then was incubated overnight at 4 °C with primary antibodies at 1: 1000 dilution. On the next day, the membrane was incubated with the secondary antibody for 2 h at room temperature. Finally, band signals were visualized using an enhanced chemiluminescence solution (Solarbio), and exposed in a ChemiDocTM XRSC system (Bio-Rad). The information of primary antibodies is as follows: anti-GPX4 (ab125066, Abcam, Cambridge, MA, USA), anti-SLC7 A11 (ab175186), anti-ALSL4 (sc-365230; Santa Cruz, CA, USA), anti-JAK2 (ab108596), anti-STAT3 (ab68153), anti-pJAK2 (ab32101), anti-p-STAT3 (ab267373), anti-GAPDH (ab8245) and anti-β-actin (ab8226).

Animal experiments

SD rats (male, 200–250 g) were provided from Charles River (Beijing, China). They allowed free access to food and water and were housed under controlled conditions (25 °C, 50% humidity, a 12-h light/dark cycle). The rats were randomly divided into five experimental groups. The normal, model, model + BMSCs, model + BMSCs + Gel matrix, and model + BMSCs + Gel matrix + colivelin groups had six animals in each group. In this work, the establishment of a fine needle punctured IVDD model: rats were anesthetized with an intraperitoneal injection of 40 mg/kg 1% pentobarbital sodium. A sterile 21 G × 1-inch needle was used to induce NP degeneration bypassing the upper region (annulus fibrosus) between the coccygeal vertebrae Co7/Co8 (cells transplanted disc) to the middle section of the disc for 30 s. The rats in the normal group maintained the same surgical time and operation steps, but the sterile needles did not penetrate the intervertebral discs, or only slightly touched the annulus fibrous without inducing degeneration. After surgery, the rats were placed in a warm environment and given plenty of food and water. One week after the initial puncture, 5 μL of colivelin at a concentration of 1 mg/mL (5 μg) was injected into the central space of the NP using a 27 G needle. The corresponding BMSCs or hydrogel mixture was injected into the IVD using the 31 G microsyringe (50 μL) after needling for 4 weeks according to the grouping.

Magnetic resonance imaging (MRI)

Four weeks after injection, the changes of NP signals in the intervertebral space were measured by MRI assay. T2-weighted imaging (T2 WI) is capable of clearly demonstrating the water content and signal intensity changes in IVD, making it a commonly used method for assessing disc degeneration. All rats underwent MRI scanning, and sagittal T2-weighted imaging was employed to obtain central images of the caudal discs (Co7-8). The signal intensity of the NP region of the IVD was measured using the image analysis software ImageJ. Specifically, regions of interest (ROIs) were delineated on the T2-weighted images, and the average signal intensity within these regions was calculated. MRI image grading refers to the improved Thomson classification. There are four levels here, the first is that the signal intensity is completely normal, the second level is a slight weakening of the signal intensity, the third level is a moderate weakening of the signal, and the fourth level is significantly

decreased signal intensity. The quantitatively measured MRI signal intensity values were classified into these four grades based on the mean and standard deviation of the signal intensity of normal IVD.

Hematoxylin and Eosin (HE) staining

Four weeks after injection, the rats were euthanized by inhalation of 5% isoflurane (Sigma-Aldrich). IVD tissue was removed from the rat IVD segment. IVD tissue was removed from the rat IVD segment. IVD was fixed in 4% paraformaldehyde for 24 h and then decalcified in a decalcified solution (14% EDTA) at 18–25 °C. The decalcified discs were dehydrated, embedded in paraffin wax, and cut into 5 μm slices. After slices dewaxing, hematoxylin was stained for 5 min and washed for 1 min. Then eosin was stained for 2 min and washed for 1 min. Finally, the slices were observed using light microscopy (Olympus, Japan) under the instructions of protocols. According to the Han Bin disc histological grading scale[17], the histological images of each group are classified into 0 to 15 scores. The higher the score, the more severe the disc degeneration. Score 5: The intervertebral disc is entirely normal, with no signs of degeneration. Scores 6–10: Mild to moderate disc degeneration, featuring reduced disc height, decreased signal intensity, structural disorganization, and endplate sclerosis. Scores 11–15: Severe degeneration, marked by significant reduction or loss of disc height, severe decrease or absence of signal intensity, extensive structural disorganization or disruption, severe endplate sclerosis or osteophyte formation, and pronounced disc herniation.

Statistical analysis

In this experiment, the sample size of the cell experiment was $n = 3$, and the sample size of the animal experiment was $n = 6$. All the experiments were performed at least three times. The data were expressed as mean ± SD and were analyzed using GraphPad Prism 7.0 (GraphPad Software Inc, San Diego, California). Additionally, the significant differences between the two independent groups were analyzed by the student's t-test. The differences between the multiple groups were compared by one-way ANOVA or two-way ANOVA followed by Tukey's post hoc test. P values < 0.05 were considered statistically significant.

Result

Identification of BMSCs

The BMSCs characteristics were detected. The ability of BMSCs to induce multiline differentiation should first be cultured in adipogenic or osteogenic medium and then analyzed by Oil red O, alizarin red, and ALP staining. Results showed that BMSCs can differentiate into osteoblasts and adipocytes (Fig. 1A-C). Flow cytometry

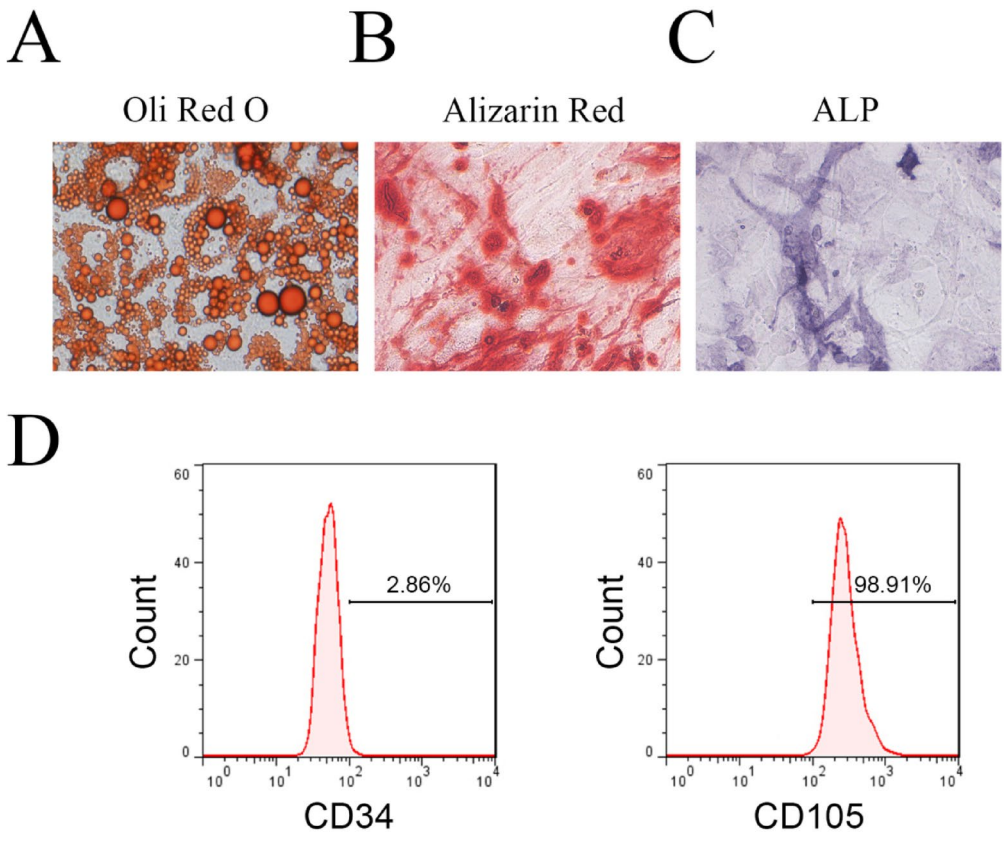

Fig. 1. Identification of BMSCs. (**A**-**C**) The ability of BMSC to differentiate into the adipogenic and osteogenic lineages was confirmed by Oil Red O staining, Alizarin Red staining, and ALP staining. (**D**) Cell surface markers (CD105 and CD34) of BMSC were detected by flow cytometric analysis.

analysis showed that BMSCs expressed the surface marker CD105 but exhibited minimal expression of CD34 (Fig. 1D).

BMSCs alleviate IVDD based on matrix hydrogels in vivo

To investigate the effect of BMSCs on IVDD progression, a rat IVDD model was established and injected with BMSCs or BMSC-embedded matrix hydrogels. Firstly, in vitro, we assessed the viability of BMSCs in the matrix hydrogel using the CCK-8 assay. The results showed that BMSCs encapsulated in the matrix hydrogel maintained high viability (Figure S1), indicating that the matrix hydrogel provides a favorable environment for BMSC survival. Subsequently, we performed an MRI to evaluate the degeneration of the NP. The normal NP tissues had more water, and the water would be decreased with the disintegration of the NP tissues. The model group showed a high MRI grade by measuring the signal intensity of the NP, indicating a low water content in the NP tissues. However, this reduced water content was reversed by BMSCs treatment, while the matrix hydrogels further increased the water content in the NP tissues. Notably, there was no statistically significant difference in MRI grading between the matrix hydrogel group and the model group (Fig. 2A-B). These findings suggested that BMSCs restored the water content of NP tissues to retard IVDD and matrix hydrogels significantly enhanced the effect of BMSCs. Next, HE staining showed that the NP cells were disordered and the NP boundary was unclear in IVDD rats, and a similar situation was observed in the rats using matrix hydrogel alone. BMSCs ameliorated the pathological condition of IVDD rats, and matrix hydrogels further enhanced this improvement (Fig. 2C-D). These results suggested that BMSCs alleviated IVDD progression based on the matrix hydrogels.

BMSCs inhibit TBHP-induced ferroptosis

Next, AFCs were treated with TBHP to establish an in vitro model and co-cultured with BMSCs to better verify the cellular biological function of BMSCs. The cell viability was decreased after the treatment of TBHP, which was increased by BMSCs treatment (Fig. 3A). Later, the LDH content, Fe^{2+}, lipid peroxidation ROS, and MDA levels were significantly increased after the treatment of TBHP, while BMSCs reversed this induction (Fig. 3B-D and F). Meanwhile, the GSH level was decreased by TBHP treatment, whereas BMSCs restored this inhibition (Fig. 3E). Finally, the results of the western blot showed that TBHP-induced down-regulation of GPX4 and SLC7 A11 levels and up-regulation of ACSL4 levels were restored by BMSCs. (Fig. 3G-J). These data indicated that BMSCs suppressed ferroptosis in AFCs treated by TBHP.

BMSCs suppress the STAT3 signal pathway

We then explored the underlying mechanism of BMSC-mediated effects on AFCs and screened the possible phosphorylated kinases and signaling nodes affected by BMSCs. The results showed that only the phosphorylation of STAT3 was reduced by BMSCs (Fig. 4A). Activation of the JAK2/STAT3 signaling pathway plays a crucial role in IVDD progression[18]and is involved in the regulation of ferroptosis[19]. We then detected STAT3 pathway-related proteins and the results suggested that the phosphorylated levels of JAK2 and STAT3 were both increased

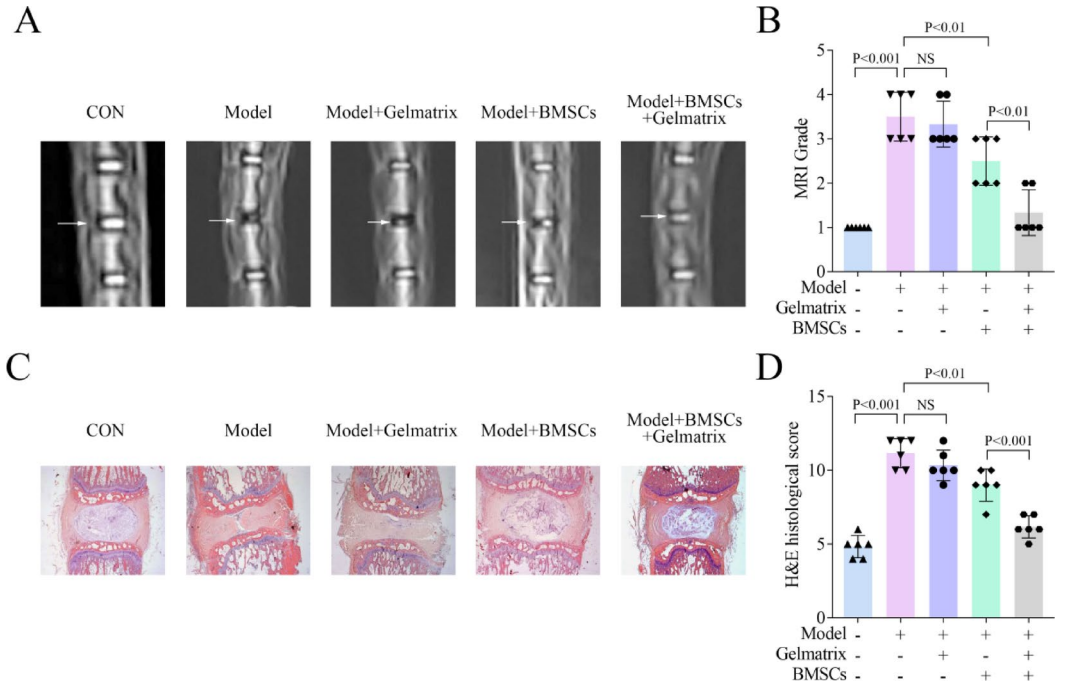

Fig. 2. BMSCs alleviate IVDD based on matrix hydrogels in vivo. (**A**) Representative MRI images of rat caudal vertebrae. The arrow points to coccygeal vertebrae Co7/Co8. (**B**) Quantitative analysis of MRI according to the Thompson score in each group. (**C**) The histopathology of the NP tissue was assessed using an HE staining assay. (**D**) The results of the HE staining assay were scored. All data are expressed as the means ± SD. ($n = 6$).

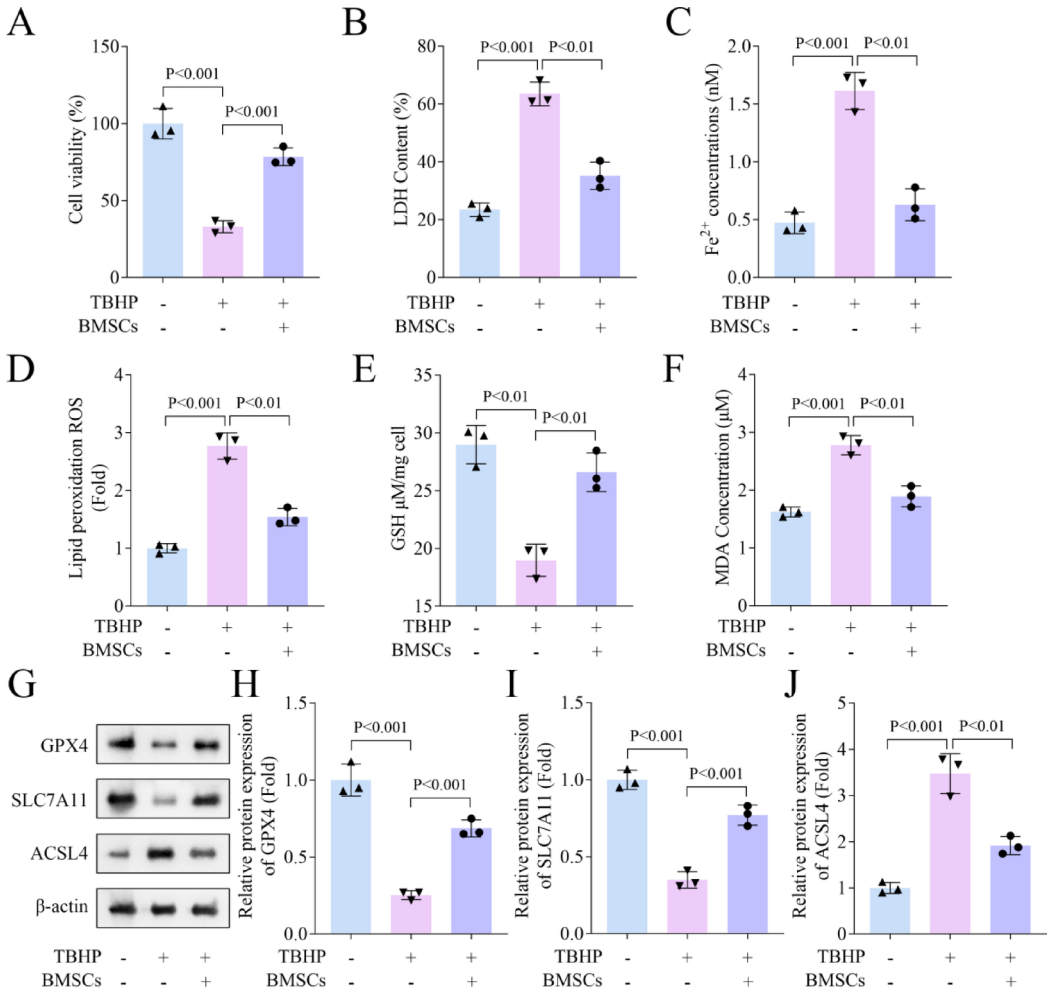

Fig. 3. BMSCs inhibit TBHP-induced ferroptosis. (**A**) Cell viability was assessed using CCK-8. (**B**) LDH content was detected using an LDH kit. (**C**-**F**) The levels of Fe^{2+}, lipid ROS, GSH, and MDA were analyzed using assay kits. (**G**-**J**) The levels of GPX4, SLC7 A11, and ACSL4 were examined using a western blot. All data are expressed as the means ± SD. ($n = 3$).

after the TBHP treatment, which was significantly decreased when co-treated with BMSCs (Fig. 4B-D). These results indicated that BMSCs inhibited the STAT3 signal pathway.

The activation of STAT3 abolishes the inhibitory effect of BMSCs on ferroptosis in TBHP-induced AFCs

To evaluate whether the biological function of BMSCs was achieved by regulating the activation of STAT3, colivelin was administered in TBHP-BMSCs co-treated AFCs to activate STAT3. The results showed that colivelin inhibited cell viability, but increased LDH content, Fe^{2+}, lipid ROS, and MDA levels in the co-cultured system (Fig. 5A-D and F). Meanwhile, colivelin reversed the upregulating effects on GSH levels induced by BMSCs treatment in TBHP-induced AFCs (Fig. 5E). Finally, the western blot showed that colivelin restored the upregulating effects on GPX4 and SLC7 A11 expression and the downregulating effect on ACSL4 expression induced by BMSCs treatment (Fig. 5G-J). These findings indicated that BMSCs inhibited TBHP-induced ferroptosis of AFCs by inhibiting the activation of STAT3.

BMSCs based on matrix hydrogels alleviate IVDD by inhibiting the activation of STAT3 in vivo

Finally, we further investigated the mechanism by which BMSCs alleviate IVDD in vivo. Based on previous studies, the BMSCs and matrix hydrogels combination treatment significantly increased the water content and improved the pathological condition of the NP tissue. However, the protective effects of BMSCs-encapsulated hydrogels on IVDD were abrogated when rats were treated with the STAT3 signaling agonist colivelin (Fig. 6A-D). These results revealed that BMSCs based on matrix hydrogels attenuated IVDD by inhibiting the activation of STAT3.

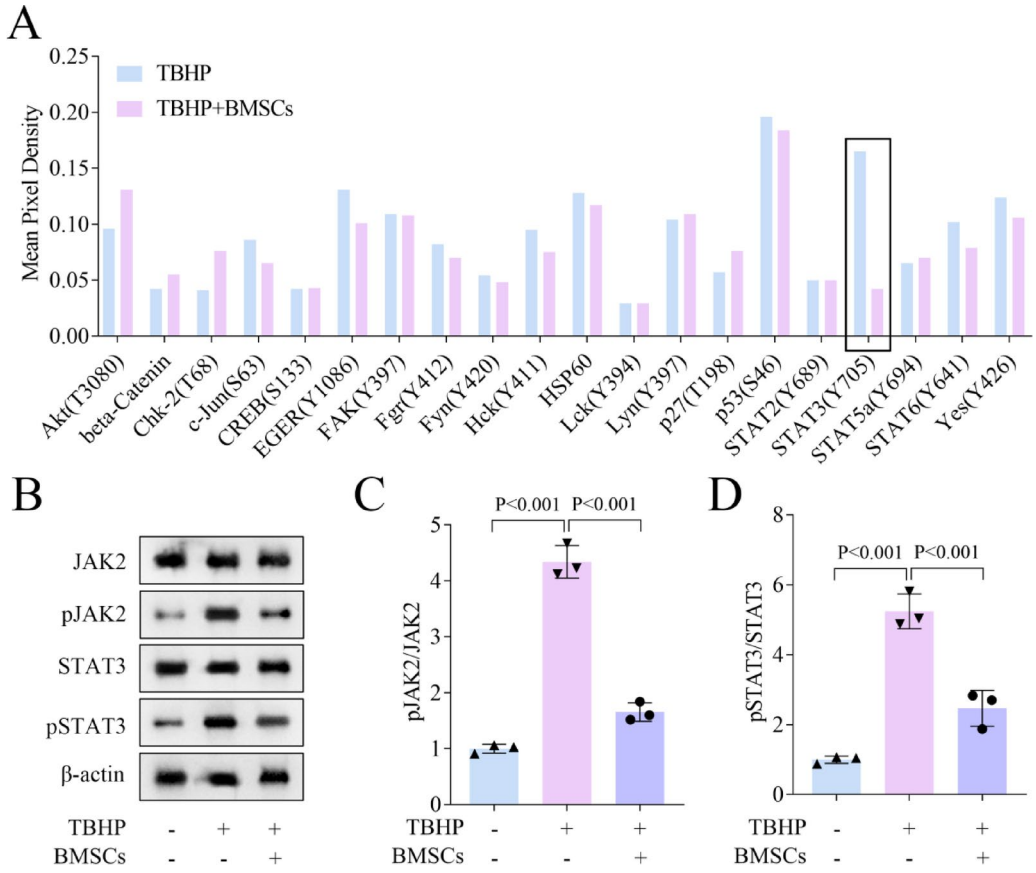

Fig. 4. BMSCs suppress the STAT3 signal pathway. (**A**) The quantified results of the phosphorylation levels of phosphorylated kinases using the human phospho-kinase array. (**B**-**D**) The levels of pJAK2, JAK2, pSTAT3, and STAT3 were examined using a western blot, and the ratios of pJAK2/JAK2 and pSTAT3/STAT3 were quantified. All data are expressed as the means ± SD. ($n = 3$).

Discussion

Among the various biological approaches, cell-based therapies appear to be the most promising technique for treating IVDD; however, it is still somewhat controversial. Cell therapy for IVDD aims to restore or replace reduced and aged NP cells in the degenerative disc. Thus, supplementing NP cells is the most direct method. However, some studies have found that NP cell transplantation loses its original differentiation ability, the ability to synthesize type II collagen, and the balance between ECM synthesis and degradation[20,21]. MSCs are an ideal cell source for the repair of disc degeneration mainly due to their similar phenotype and multidirectional differentiation ability to natural NP cells[22,23]. In our work, we explored the effect of BMSCs on IVDD and its related mechanisms.

A normal intervertebral disc comprises the central gelatinous NP, the outer AF, and the adjacent vertebral bodies connected through the cartilage endplate. AF is important for maintaining the position and shape of the NP, as well as the integrity of the ECM[24]. The death of AFCs accelerates the progression of IVDD[25]. Ferroptosis is a special cell death induced by oxidative stress and is usually accompanied by iron accumulation, lipid peroxidation, glutathione system depletion, and the formation and release of ROS during the cell death process. The interplay between ferroptosis and oxidative stress has occurred frequently in many diseases, such as stroke[26], Alzheimer's disease[27], and IVDD[28]. For instance, inhibition of ferroptosis induced by oxidative stress can alleviate IVDD[29]. On the contrary, elevated levels of ferroptosis marker protein (GPX4, TFR1, and SCL7 A11) and lipid peroxidation in TBHP-induced oxidative stress cells lead to the degeneration of IVD cells, thereby aggravating IVDD[30]. Of note, ferroptosis inhibitors can significantly alleviate IVDD, suggesting that ferroptosis is a novel therapeutic target for IVDD[31].

It is worth noting that inhibition of oxidative stress-induced AFCs ferroptosis during the process of IVDD can reduce the degree of disc degeneration[32]. In this work, we treated AFCs with TBHP to simulate the oxidative stress response in IVDD. Then, we found that ferroptosis occurred in AFCs treated with TBHP, while BMSCs significantly inhibited ferroptosis, indicating that BMSCs can alleviate IVDD by suppressing the ferroptosis of AFCs. Next, we explored the specific molecular mechanisms and used a proteome profiler to reveal possible signaling nodes that are affected by BMSCs. We observed that BMSCs significantly downregulated the phosphorylation levels of STAT3 in TBHP-induced AFCs. Not only that, but BMSCs also reduced the phosphorylation of JAK2, suggesting that BMSCs served functions through the JAK2/STAT3 signaling axis.

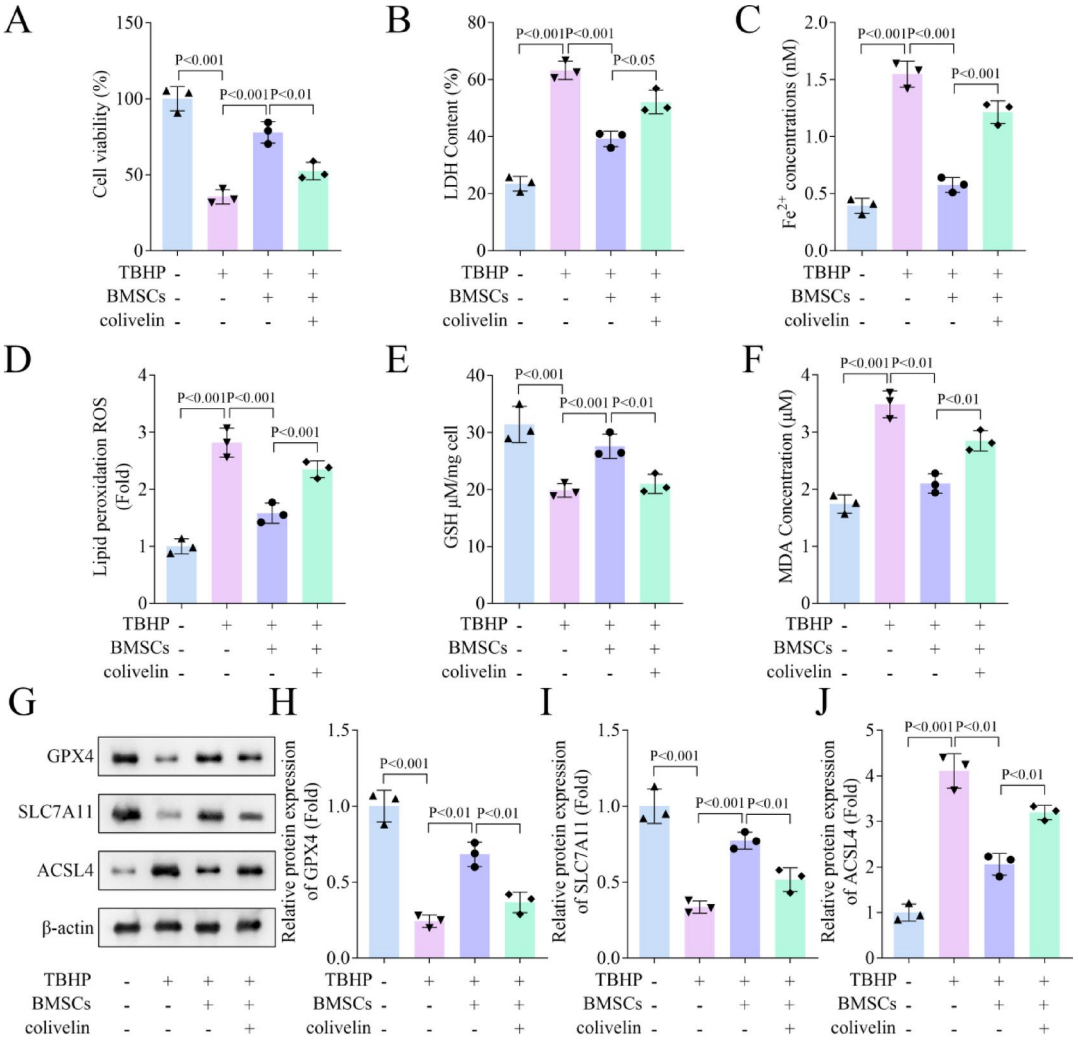

Fig. 5. The activation of STAT3 abolishes the inhibitory effect of BMSCs on ferroptosis in TBHP-induced AFCs. (**A**) Cell viability was assessed using CCK-8. (**B**) LDH content was detected using an LDH kit. (**C**-**F**) The levels of Fe^{2+}, lipid ROS, GSH, and MDA were analyzed using assay kits. (**G**-**J**) The levels of GPX4, SLC7 A11, and ACSL4 were examined using a western blot. All data are expressed as the means ± SD. ($n = 3$).

STAT3 is a cytoplasmic transcription factor of the mammalian STAT family and is also a valued member of the JAK/STAT signaling pathway[33]. It is involved in a variety of biological processes such as cell proliferation, differentiation, survival, and angiogenesis[34]. STAT3 can be activated to perform its function by inducing phosphorylation of tyrosine (705) and serine (727) residues via its upstream ligand, JAK2[35]. In addition, the JAK2/STAT3 signaling pathway is relevant to the onset and progression of diseases, such as neurological disease[36], immune-inflammatory diseases[37], and cancer[38]. A study has shown that the inhibition of the JAK2/STAT3 signaling pathway suppresses apoptosis and ECM degradation, but promotes autophagy and the function of NPCs in IVDD[39]. Negative regulation of the JAK2/STAT3 phosphorylation and the decreased IL-6 expression can ameliorate IVDD[40]. Interestingly, phosphorylated STAT3 upregulation contributes to ferroptosis by increasing NCOA4 expression[41]. Consistent with these studies is that in our study, we treated cells with colivelin to specifically activate STAT3 and found that it abolished the inhibitory effect of BMSCs on TBHP-induced ferroptosis of AFCs, suggesting that activation of STAT3 canceled the protective effect of BMSCs against IVDD.

Finally, to investigate the impact of BMSCs on IVDD progression in vivo, we constructed the rat IVDD model by needle puncturing. Notably, hydrogels can act as delivery vectors for MSCs, not only promoting extracellular matrix production and cell viability but also providing a microenvironment conducive to cell survival. At present, hydrogels have been widely used in 3D cell culture and clinical research. In addition, modified hydrogels have more advantages in effectively maintaining cell viability, such as plasma, cytokine, and costal cartilage extracellular matrix[42–44]. A previous study has revealed that BMSCs alleviate IVDD induced by LPS in vivo based on matrix hydrogels[45]. Consistent with this research, here we found that BMSCs increased the water content of the NP tissues and mitigated the histopathology of IVDD. Meanwhile, the effect of BMSCs is further enhanced with BMSC-encapsulated hydrogel treatment in vivo. Importantly, the protective effects of

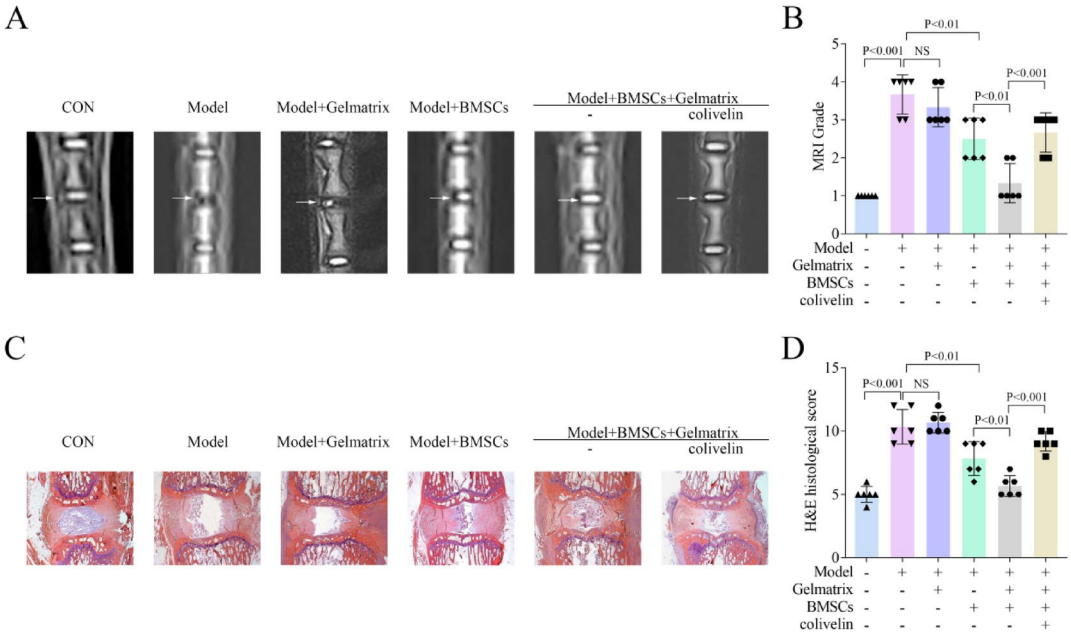

Fig. 6. BMSCs based on matrix hydrogels alleviate IVDD by inhibiting the activation of STAT3 in vivo. (**A**) Representative MRI images of rat caudal vertebrae. The arrow points to coccygeal vertebrae Co7/Co8. (**B**) Quantitative analysis of MRI according to the Thompson score in each group. (**C**) The histopathology of the NP tissue was assessed using an HE staining assay. (**D**) The results of the HE staining assay were scored. All data are expressed as the means ± SD. ($n = 6$).

BMSCs-encapsulated hydrogels on IVDD were abrogated by colivelin treatment, indicating that BMSCs retard IVDD progression by inhibiting the activation of STAT3.

In short, we found that BMSCs alleviated IVDD progression in vivo, and inhibited oxidative stress-induced AFCs ferroptosis by inhibiting the activation of STAT3 in vitro. The therapeutic effects of BMSCs were further enhanced by matrix hydrogels. These findings support the role of ferroptosis in the pathogenesis of IVDD and provide evidence for a potential therapeutic strategy for IVDD.

Data availability

The datasets used and/or analysed during the current study are available from the corresponding author on reasonable request.

Received: 22 August 2024; Accepted: 28 April 2025
Published online: 02 May 2025

References

1. Manchikanti, L., Singh, V., Falco, F. J., Benyamin, R. M. & Hirsch, J. A. Epidemiology of low back pain in adults. *Neuromodulation* **17** (Suppl 2), 3–10 (2014).
2. Roberts, S., Evans, H., Trivedi, J. & Menage, J. Histology and pathology of the human intervertebral disc. *J. Bone Joint Surg. -Am Vol.* **88** (Suppl 2), 10–14 (2006).
3. Yavin, D. et al. Lumbar fusion for degenerative disease: A systematic review and Meta-Analysis. *Neurosurgery* **80**, 701–715 (2017).
4. Roh, E. J. et al. Genetic therapy for intervertebral disc degeneration. *Int. J. Mol. Sci.* **22**(4), 1579 (2021).
5. Hu, B. et al. Intervertebral disc-Derived stem/progenitor cells as a promising cell source for intervertebral disc regeneration. *Stem Cells Int.* **2018**, 7412304 (2018).
6. Kozlowska, U. et al. Similarities and differences between mesenchymal stem/progenitor cells derived from various human tissues. *World J. Stem Cells*. **11**, 347–374 (2019).
7. Vadala, G., Russo, F., Ambrosio, L., Loppini, M. & Denaro, V. Stem cells sources for intervertebral disc regeneration. *World J. Stem Cells*. **8**, 185–201 (2016).
8. Hu, S. et al. Mesenchymal Stem Cell-Derived Extracellular Vesicles: Immunomodulatory Effects and Potential Applications in Intervertebral Disc Degeneration. *Stem Cells Int.* 7538025 (2022). (2022).
9. Vizoso, F. J. et al. Mesenchymal stem cells in homeostasis and systemic diseases: Hypothesis, evidences, and therapeutic opportunities. *Int. J. Mol. Sci.* **20**(15), 3738 (2019).
10. Richardson, S. M. et al. Mesenchymal stem cells in regenerative medicine: focus on articular cartilage and intervertebral disc regeneration. *Methods* **99**, 69–80 (2016).
11. Buckley, C. T. et al. Critical aspects and challenges for intervertebral disc repair and Regeneration-Harnessing advances in tissue engineering. *Jor Spine*. **1**, e1029 (2018).
12. Wang, F. et al. Injectable Hydrogel Combined with Nucleus Pulposus-Derived Mesenchymal Stem Cells for the Treatment of Degenerative Intervertebral Disc in Rats. *Stem Cells Int.* 1–17 (2019). (2019).
13. Borde, B., Grunert, P., Härtl, R., Bonassar, L. J. & Injectable High-Density collagen gels for annulus fibrosus repair: an in vitro rat tail model. *J. Biomed. Mater. Res. A*. **103**, 2571–2581 (2015).
14. Chaudhuri, O. et al. Hydrogels with tunable stress relaxation regulate stem cell fate and activity. *Nat. Mater.* **15**, 326–334 (2016).

15. Smith, L. J. et al. In vitro characterization of a Stem-Cell-Seeded Triple-Interpenetrating-Network hydrogel for functional regeneration of the nucleus pulposus. *Tissue Eng. Part A*. **20**, 1841–1849 (2014).
16. Roughley, P. et al. The potential of Chitosan-Based gels containing intervertebral disc cells for nucleus pulposus supplementation. *Biomaterials* **27**, 388–396 (2006).
17. Han, B. et al. A simple disc degeneration model induced by percutaneous needle puncture in the rat tail. *Spine* **33**, 1925–1934 (2008).
18. Miao, D. & Zhang, L. Leptin modulates the expression of catabolic genes in rat nucleus pulposus cells through the Mitogen-Activated protein kinase and Janus kinase 2/signal transducer and activator of transcription 3 pathways. *Mol. Med. Rep.* **12**, 1761–1768 (2015).
19. Zhao, Y. et al. Chlorogenic acid alleviates chronic Stress-Induced duodenal ferroptosis via the Inhibition of the Il-6/Jak2/Stat3 signaling pathway in rats. *J. Agric. Food Chem.* **70**, 4353–4361 (2022).
20. Mwale, F. et al. Effect of a type Ii collagen fragment on the expression of genes of the extracellular matrix in cells of the intervertebral disc. *open. Orthop. J.* **2**, 1–9 (2008).
21. Huang, S. et al. Stem Cell-Based approaches for intervertebral disc regeneration. *Curr. Stem Cell. Res. Ther.* **6**, 317–326 (2011).
22. Risbud, M. V. et al. Differentiation of mesenchymal stem cells towards a nucleus Pulposus-Like phenotype in vitro: implications for Cell-Based transplantation therapy. *Spine* **29**, 2627–2632 (2004).
23. Ohnishi, T. et al. A Review: Methodologies to Promote the Differentiation of Mesenchymal Stem Cells for the Regeneration of Intervertebral Disc Cells Following Intervertebral Disc Degeneration. *Cells*. 12, (2023).
24. Smith, L. J., Nerurkar, N. L., Choi, K., Harfe, B. D. & Elliott, D. M. Degeneration and regeneration of the intervertebral disc: lessons from development. *Dis. Model. Mech.* **4**, 31–41 (2011).
25. Yang, F. et al. Regulated cell death: implications for intervertebral disc degeneration and therapy. *J. Orthop. Transl.* **37**, 163–172 (2022).
26. Ren, J. X. et al. Crosstalk Between Oxidative Stress and Ferroptosis/Oxytosis in Ischemic Stroke: Possible Targets and Molecular Mechanisms. *Oxidative Med. Cell. Longev.* 6643382 (2021). (2021).
27. Park, M. W. et al. Nox4 promotes ferroptosis of astrocytes by oxidative Stress-Induced lipid peroxidation via the impairment of mitochondrial metabolism in Alzheimer's diseases. *Redox Biol.* **41**, 101947 (2021).
28. Wang, W. et al. Iron overload promotes intervertebral disc degeneration via inducing oxidative stress and ferroptosis in endplate chondrocytes. *Free Radic Biol. Med.* **190**, 234–246 (2022).
29. Zhu, J. et al. The deubiquitinase Usp11 ameliorates intervertebral disc degeneration by regulating oxidative Stress-Induced ferroptosis via deubiquitinating and stabilizing Sirt3. *Redox Biol.* **62**, 102707 (2023).
30. Fan, C. et al. The role of ferroptosis in intervertebral disc degeneration. *Front. Cell. Dev. Biol.* **11**, 1219840 (2023).
31. Zhou, L. P. et al. Ferroptosis: A potential target for the intervention of intervertebral disc degeneration. *Front. Endocrinol.* **13**, 1042060 (2022).
32. Yang, R. Z. et al. Involvement of oxidative Stress-Induced annulus fibrosus cell and nucleus pulposus cell ferroptosis in intervertebral disc degeneration pathogenesis. *J. Cell. Physiol.* **236**, 2725–2739 (2021).
33. Darnell, J. J., Kerr, I. M. & Stark, G. R. Jak-Stat pathways and transcriptional activation in response to Ifns and other extracellular signaling proteins. *Science* **264**, 1415–1421 (1994).
34. Galoczova, M., Coates, P. & Vojtesek, B. Stat3, stem cells, Cancer stem cells and P63. *Cell. Mol. Biol. Lett.* **23**, 12 (2018).
35. Sgrignani, J. et al. Structural biology of Stat3 and its implications for anticancer therapies development. *Int. J. Mol. Sci.* **19**(6), 1591 (2018).
36. Hu, Z. et al. Cntf-Stat3-Il-6 Axis mediates neuroinflammatory cascade across Schwann Cell-Neuron-Microglia. *Cell. Rep.* **31**, 107657 (2020).
37. Zhu, L. et al. Stat3/Mitophagy Axis coordinates macrophage Nlrp3 inflammasome activation and inflammatory bone loss. *J. Bone Min. Res.* **38**, 335–353 (2023).
38. Fan, Y., Mao, R. & Yang, J. Nf-Kappab and Stat3 signaling pathways collaboratively link inflammation to Cancer. *Protein Cell.* **4**, 176–185 (2013).
39. Bai, X. et al. Cyanidin attenuates the apoptosis of rat nucleus pulposus cells and the degeneration of intervertebral disc via the Jak2/Stat3 signal pathway in vitro and in vivo. *Pharm. Biol.* **60**, 427–436 (2022).
40. Xu, H. W. et al. Alpha-Ketoglutaric acid ameliorates intervertebral disk degeneration by blocking the Il-6/Jak2/Stat3 pathway. *Am. J. Physiol. -Cell Physiol.* **325**, C1119–C1130 (2023).
41. Zhu, M. et al. Stat3 signaling promotes cardiac injury by upregulating Ncoa4-Mediated ferritinophagy and ferroptosis in High-Fat-Diet fed mice. *Free Radic Biol. Med.* **201**, 111–125 (2023).
42. Samberg, M. et al. Platelet rich plasma hydrogels promote in vitro and in vivo angiogenic potential of Adipose-Derived stem cells. *Acta Biomater.* **87**, 76–87 (2019).
43. Böck, T. et al. Tgf-B1-Modified hyaluronic Acid/Poly(Glycidol) hydrogels for chondrogenic differentiation of human mesenchymal stromal cells. *Macromol. Biosci.* **18**, e1700390 (2018).
44. Luo, L. et al. Injectable cartilage matrix hydrogel loaded with cartilage endplate stem cells engineered to release exosomes for Non-Invasive treatment of intervertebral disc degeneration. *Bioact Mater.* **15**, 29–43 (2022).
45. Sang, P., Li, X. & Wang, Z. Bone mesenchymal stem cells inhibit oxidative Stress-Induced pyroptosis in annulus fibrosus cells to alleviate intervertebral disc degeneration based on matric hydrogels. *Appl. Biochem. Biotechnol.* **196**(11), 8043–8057 (2024).

Acknowledgements

Not applicable.

Author contributions

All authors participated in the design, interpretation of the studies and analysis of the data and review of the manuscript. S F drafted the work and revised it critically for important intellectual content; R L, L W, Z W, F W, H G, W Z, X H and X L were responsible for the acquisition, analysis and interpretation of data for the work; Y W made substantial contributions to the conception or design of the work. All authors read and approved the final manuscript.

Funding

The work was supported by Joint TCM Science &Technology Projects of Nationa1 Demonstration Zones for Comprehensive TCM Reform under grant number GZY-KJS-SD-2023-031.

Declarations

Competing interests
The authors declare no competing interests.

Ethics approval and consent to participate
This study was approved by the Ethics Committee of Shandong Wendeng Orthopedic Hospital. All animal experiments should comply with the ARRIVE guidelines. All methods were carried out in accordance with relevant guidelines and regulations.

Additional information
Supplementary Information The online version contains supplementary material available at https://doi.org/10.1038/s41598-025-00278-x.

Correspondence and requests for materials should be addressed to Y.W.

Reprints and permissions information is available at www.nature.com/reprints.

Publisher's note Springer Nature remains neutral with regard to jurisdictional claims in published maps and institutional affiliations.